Excitonic molecule in a quantum dot: Photoluminescence lifetime of a single InAs/GaAs quantum dot

Shunsuke Kono,[1,3,*] Akihiro Kirihara,[1,3] Akihisa Tomita,[1,3,4] Kazuo Nakamura,[1,3,†] Junichi Fujikata,[1] Keishi Ohashi,[1] Hideaki Saito,[2] and Kenichi Nishi[1]

[1]*Fundamental and Environmental Research Laboratories, NEC Corporation, 34 Miyukigaoka, Tsukuba 305-8501, Japan*

[2]*System Device Research Laboratories, NEC Corporation, 1120 Shimokuzawa, Sagamihara 229-1198, Japan*

[3]*CREST, Japan Science and Technology Agency, 4-1-8 Honcho, Kawaguchi 332-0012, Japan*

[4]*ERATO, Japan Science and Technology Agency, 4-1-8 Honcho, Kawaguchi 332-0012, Japan*

(Received 27 April 2005; revised manuscript received 17 August 2005; published 12 October 2005)

Time dependence of the photoluminescence (PL) attributed to the exciton and biexciton in a single InAs/GaAs quantum dot is investigated at 4.3 K with microscopic spectroscopy. Dynamical behavior of the PL decay and the excitation intensity dependence of the exciton and biexciton PL are analyzed by rate equations assuming a cascading recombination from the biexciton to exciton state. The analysis shows that the biexciton lifetime is longer than the exciton lifetime. The estimated ratio of the biexciton lifetime to the exciton lifetime shows a molecular nature of the biexciton in the large quantum dots compared with the exciton Bohr radius.

DOI: 10.1103/PhysRevB.72.155307 PACS number(s): 71.35.−y, 78.47.+p, 78.67.Hc

I. INTRODUCTION

Optical properties of semiconductor quantum dots have been studied extensively, in anticipation of various potential applications for optoelectronic devices. Delta-functionlike density of states in a quantum dot shows many interesting properties due to the strong quantum confinement of electron-hole pairs. One of the properties that has attracted widespread attention is one in which photons radiated from a single exciton system in a single quantum dot show nonclassical statistics, called antibunching.[1,2] This nonclassical nature of light originating from this nanostructured semiconductor material plays an important role in quantum information technology as shown by the quantum optical experiments with the single photon sources using semiconductor quantum dots.[3,4]

Single photon sources at the communication wavelength are currently being explored by the spectroscopic studies on single quantum dots in the wavelength range longer than 1 μm.[5–8] Besides such practical interests, InAs self-assembled quantum dots having a longer resonance wavelength are expected to show interesting properties such as large exciton binding energy and large energy separation between the quantized levels because the confined levels in these dots are deep compared with the continuum level in the wetting layer.

In this paper, we have measured the time dependences of the photoluminescence (PL) intensities attributed to the exciton and biexciton in a single InAs/GaAs quantum dot at the wavelength 1.18 μm by using a time-correlated single photon counting technique. Coulomb interaction enhanced by the strong confinement in the quantum dot will affect the wave function of the multiexciton state. Thus the dynamical investigation on the exciton and biexciton in the single quantum dots having the longer resonant wavelength is interesting since such dynamical investigations have been mainly performed with quantum dots of smaller confinement typically represented by InAs quantum dots having a resonance wavelength shorter than 1 μm.[9]

We analyzed the observed temporal behaviors of the PL intensities by a simple rate equation model by assuming the cascade emission process from biexciton to exciton. The same rate equation model was used to analyze the excitation intensity dependence of the ratio of the biexciton PL intensity to exciton PL intensity. As a result of the rate equation analysis, we found that the ratio of the radiative lifetime of the exciton τ_X, to that of the biexciton τ_B, was less than 1.

The ratio τ_X/τ_B is expected to be equal to 2 when the constituent excitons of a biexciton are independent. However, due to the quantum confinement and dielectric confinement in nanostructures, this ratio was theoretically predicted to be smaller than 2.[10,11] This deviation was experimentally observed in CdSe quantum dots by Bacher *et al.*, where they found that τ_X was slightly shorter than τ_B.[12] Santori *et al.* reported the ratio about 1.5 in InAs quantum dots at the wavelength of 0.88 μm.[9] The obtained ratio in our report is consistent with the discussion in these reports and theoretical predictions by taking into account the difference in the confinement energy and quantum dot dimensions.

II. EXPERIMENTS

The InAs quantum dots were grown on the (001) GaAs surface by molecular beam epitaxy at 590 °C. The quantum dot layer was capped with 150-nm-thick GaAs layer. The quantum dot sample grown with the same condition without a capping layer was separately prepared to estimate the topographic information of the quantum dot growth. The average diameter and height of the quantum dots were estimated to be 49 and 13 nm respectively using an atomic force microscope. The dot density was less than 10^{10} dots/cm^2. In order to reduce the number of the quantum dots in the focusing area of a microscope, we fabricated metal mask apertures on the sample. The apertures were fabricated on the 100-nm-thick Au layer by electron beam lithography and a lift-off technique. The diameters of the apertures were 0.4, 0.6, 0.8, and 1.0 μm. The sample was cooled down to 4.3 K in the

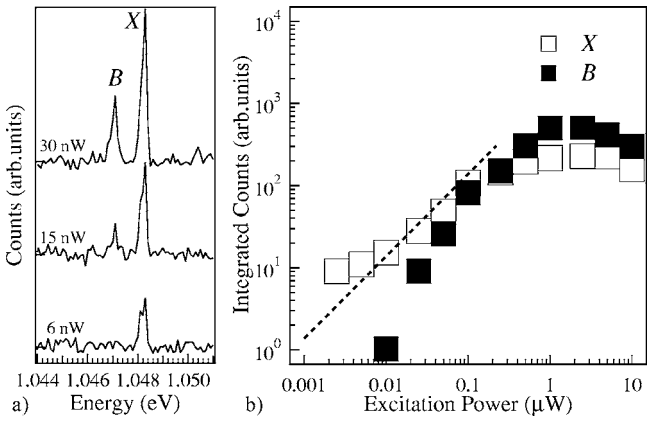

FIG. 1. (a) PL spectra of a single quantum dot observed through 0.6-μm-diameter metal mask aperture at different excitation intensities. Peak labeled with *X* is attributed to the exciton recombination, peak labeled *B* to the biexciton recombination. (b) Integrated intensities of peak *X* (open square) and *B* (filled square) as a function of the excitation power intensity. Dashed line is linear to the excitation intensity.

conduction type microscope cryostat mounted on a piezo-actuated translation stage for sample positionning.

One of the microapertures was selected with a laboratory-made confocal microscope and illuminated by excitation lasers through an objective lens (numerical aperture=0.42) that was at the same time used to collect luminescence from the observed aperture. The image of the sample surface was formed on one of the ends of a single-mode optical fiber which extract the area of ϕ=5 μm on the sample. The sample surface was monitored by a video-charge-coupled device (CCD) camera and this image was used to stabilize the sample position by the piezo-actuated translation stage. The accuracy of sample positioning was less than 0.2 μm over three hours of signal accumulation. The PL collected with the single-mode optical fiber was introduced into a single monochromator (f=640 mm) with a liquid nitrogen-cooled InGaAs multichannel detector (Jobin-Yvon IGA-512) and liquid nitrogen-cooled photomultiplier (PMT, Hamamatsu R5509-42). The InGaAs multichannel detector was used to obtain overall PL spectra while the InGaAs PMT was used for time-correlated single photon counting.

III. RESULTS AND DISCUSSIONS

Figure 1(a) shows the PL spectra of a single InAs/GaAs quantum dot observed through a ϕ=0.6-μm-diameter metal mask aperture under band-to-band excitation with a He-Ne laser at different excitation intensities. At weak excitation, a single PL peak was observed at the energy of 1.0483 eV in the lowest trace of Fig. 1(a). This peak shows a small doublet structure, suggesting the exciton splitting due to the asymmetry of the quantum dot introduced by anisotropy of the shape or internal strains. With increasing excitation intensity, while the intensity of this peak grew proportionally to the excitation intensity, an additional PL peak appeared at 1.0471 eV in addition to the peak labeled *X*. We label this additional peak *B*.

In Fig. 1(b), the integrated intensities of peaks *X* and *B* in Fig. 1(a) are plotted as a function of the excitation intensity of the He-Ne laser. In the weak excitation intensity range, the intensity of the PL peak *X*, represented by open squares, is proportional to the excitation intensity. The integrated intensity of the PL peak *B*, represented by filled squares, is proportional to the square of the excitation intensity. The analysis on the excitation intensity dependence shows that peak *X* is attributed to the exciton recombination, and peak *B* attributed to the biexciton recombination. The separation of these peaks gave a biexciton binding energy estimated to be 1.2 meV.

The resonance wavelengths of the first and higher excited states in our quantum dot samples are quite similar to those reported by Kaiser *et al.*[5] However, the diameter of their quantum dots ranged from 15 to 20 nm, more than two times smaller than the average diameter of our sample. Their quantum dots were grown on the thin layer of $In_{0.15}Ga_{0.85}As$, thus the internal strain was smaller than our samples that were grown on the GaAs substrate. Introducing larger strain in InAs/GaAs quantum dots compensated for the smaller confinement effect in larger quantum dots. The similarity of the energy structures between their samples and ours are due to the compensation effects of size and strain.

While the energy levels are quite similar to each other, the biexciton binding energy estimated in Kaiser report was about 3.5 meV about three times larger than our estimation of 1.2 meV. According to the theories in Refs. 11 and 13, increasing the quantum dot diameter decreases the biexciton binding energy. Thus the observed difference in the biexciton binding energy is mainly due to the difference in the diameter of the quantum dots.

In order to investigate dynamical behavior of the PL decay of the exciton and biexciton in the single quantum dot, the same metal mask aperture measured in Fig. 1 was irradiated with a ps mode-locked Ti:Sapphire laser. The pulse duration and repetition rate were 4 ps and 100 MHz respectively. The time-correlated single photon counting technique was adopted to measure the time dependence of the PL intensity. The current pulses converted from the luminescence photons in the PMT started a time-correlated single photon counting board (PicoQuant TimeHarp200) and trigger pulses from a PIN photo diode monitoring a portion of the excitation pulses stopped the time-correlated counting board. The response time of the total detection system was estimated to be 1 ns. The upper and lower traces in Fig. 2(a) show the time-dependent intensities of the PL corresponding to the peaks labeled *B* and *X* in Fig. 1(a), respectively, at the average excitation power of 60 nW, corresponding to the pulse energy of 0.6 fJ. The traces shown in Fig. 2(b) were the signals obtained at the different excitation power. In the case of Fig. 2(a), the actual photon number incident into the aperture was estimated to be 50 photons per pulse by considering the nominal ratio of the excitation laser spot size to the aperture size. Each trace in Fig. 2 was obtained after 3 hrs of signal accumulation. The observed photon flux was estimated to be 20 photons per second for the upper trace in Fig. 2(a).

The transition from the biexciton to the exciton is accompanied with the radiative recombination of any constituent

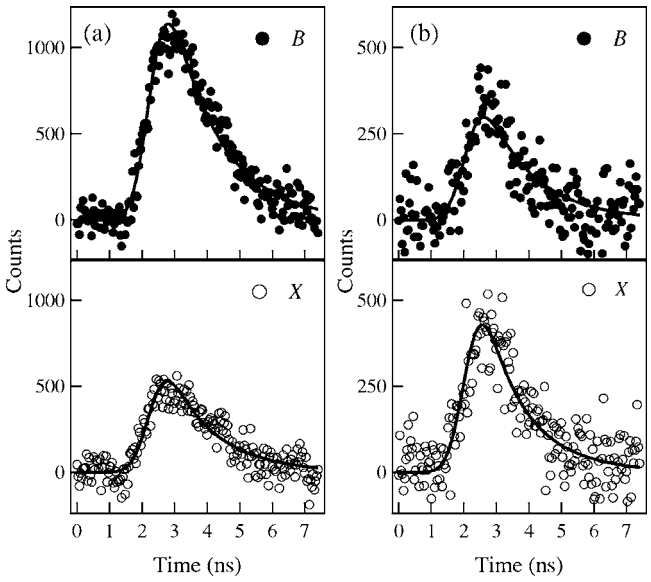

FIG. 2. Time-resolved luminescence intensities of PL peak B (filled circles) and X (open circles) at the excitation intensity of 60 nW [column (a)], and 30 nW [column (b)]. Solid curves represent the numerical solutions of the coupled rate equations explained in the manuscript.

exciton of the biexciton resulting in the rest of the constituent exciton left behind. The cascade recombination processes starting from the biexciton to the crystal ground state are explained by the coupled differential equations as follows:[12]

$$\frac{dp_B}{dt} = -\frac{p_B}{\tau_B}, \tag{1}$$

$$\frac{dp_X}{dt} = -\frac{p_X}{\tau_X} + \frac{p_B}{\tau_B}. \tag{2}$$

p_X and p_B denote the population probabilities of the exciton and biexciton levels, respectively. τ_X and τ_B represent the radiative lifetime of the biexciton state and exciton state respectively.

We ignored the effects of the higher excited states and charged exciton states in the above rate equations. Especially for higher excited states, that is, multiexciton states of the exciton number larger than 3, we did not observe the PL peaks corresponding to the higher excited state of the principal quantum number $n=2$ under the pulsed excitation with the same excitation intensity of Fig. 2(a).

The rate equations show that the radiative lifetime of the biexciton τ_B can be estimated by a single exponential fitting. Including the convolution of the response function of the detection system, τ_B was estimated to be 1.5 ± 0.2 ns according to the upper trace of Fig. 2(a). The response function of the total detection system was approximated with a Gaussian function whose width was 1 ns. Using the estimated τ_B, the coupled rate equations were solved numerically with various combinations of τ_X and ratio of the initial populations at $t=0$, p_{B0}/p_{X0}. We tried to find an appropriate numerical solution that reproduces the PL decay curve of the peak X by the least squares method. The parameters corresponding to the derived numerical solution gave the exciton lifetime τ_X and initial population ratio of the exciton and biexcitons. The solid curves in Fig. 2(a) shows numerical solutions giving $\tau_X=0.5$ ns and $p_{B0}/p_{X0}=2.08$ with the estimated value of $\tau_B=1.5$ ns. These numerical analyses show that the biexciton lifetime is estimated to be three times longer than the exciton lifetime.

At the excitation power where the numerical analysis was made for the traces in Fig. 2(a), peak X showed a slight saturation effect while peak B was still proportional to the square of the excitation intensity. Figure 2(b) shows the time dependence of the PL intensity of the same peaks X and B at the weak excitation intensity of 30 nW where no saturation effect was observed for either of the PL peaks. Due to the poor signal-to-noise ratio of the upper trace of Fig. 2(b), we used the same τ_B estimated in Fig. 2(a) for the numerical solution of the rate equations. The solid curves in Fig. 2(b) represent the numerical solution of the rate equation analysis, giving $\tau_X=0.8$ ns and $p_{B0}/p_{X0}=0.63$. At the excitation intensity in the linear regime, the ratio τ_X/τ_B is close to 1/2.

As mentioned before, we did not observe PL peaks corresponding to the higher excited states of the single quantum dot in a time-integrated PL spectrum under band-to-band excitation. The energy relaxation of the electron-hole pairs could be rapid enough so that the radiative recombination of the higher excited states was not observed. Thus we assumed that the exciton and biexciton were initially populated within a short enough period just after the optical excitation.

Under the band-to-band excitation, the electrons and holes created in the layers surrounding the quantum dots will be captured into the dot potentials after a finite relaxation time. We have assumed this capturing time was short enough to be ignored. However, Santori *et al.* discussed this finite capturing time under the above-band excitation and cited 0.2 ns as a capturing time.[9] The response time of our detection system was much longer than this capturing time so that the building up of the exciton-biexciton population could not be resolved in the time-dependent PL signals. This limited response time of our detection system also prevented us from resolving a long delayed rise of the exciton PL that was typically observed as a plateaulike characteristics of the exciton PL in Ref. 12.

We applied the above rate equation analysis to explain the ratio of the integrated PL intensity of the biexciton, I_B, to that of the exciton, I_X. The traces in Fig. 3 are the numerical estimation of the ratio of I_B/I_X as a function of the initial ratio of the population probabilities of p_{B0}/p_{X0}, with different ratios of the exciton lifetime to biexciton lifetime, τ_X/τ_B. The ratios of the integrated intensity, I_B/I_X, corresponding to Figs. 2(a) and 2(b), are shown by circles in Fig. 3, respectively indicated by a and b. These observed ratios were reproduced with the solid curve shown in Fig. 3 with $\tau_X/\tau_B=0.33$, which corresponds to the estimation of the lifetimes, with $\tau_B=1.5$ ns and $\tau_X=0.5$ ns. On the other hand, the dotted curve is a numerical estimation with $\tau_X/\tau_B=2$, and I_B/I_X approaches 1/2 as the initial population ratio is increased. The observed excitation intensity dependence shows that the ratio of the biexciton PL intensity to the exciton PL intensity exceeded even 2 when the initial population ratio was increased. The ratio of the lifetimes estimated by the rate equa-

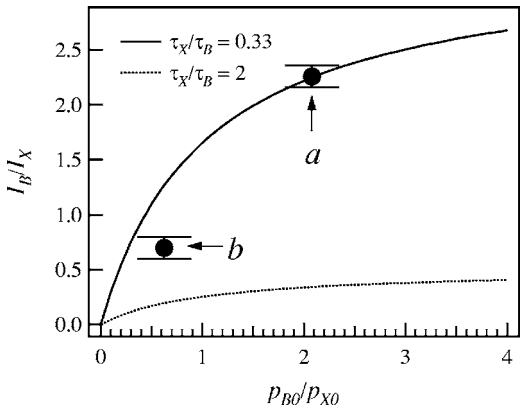

FIG. 3. Ratio of the integrated PL intensity of biexciton to that of exciton as a function of the initial ratio of the population probability p_{B0}/p_{X0}. Solid and dotted curves correspond to the cases where $\tau_X/\tau_B=0.33$ and 2, respectively. Filled circles represent I_B/I_X estimated according to Fig. 2(a) (indicated by *a*) and 2(b) (indicated by *b*).

tion analysis in this paper consistently explains the excitation intensity dependence of the exciton and biexciton PL intensity. The excitation intensity dependence of the PL peaks in Fig. 1(b) shows that the PL intensity of peak *B* exceeds that of the *X* at the excitation power where peak *B* shows the saturation effect. This similar behavior observed under continuous wave excitation is also explained by the estimated ratio of the lifetimes.

The ratio of the radiative lifetime of excitons to that of biexcitons is intuitively understood by a simple argument that the radiative recombination of any of constituent excitons of a biexciton occurs twice as often as than that of a single exciton. This argument gives $\tau_X/\tau_B=2$. However, the deviation from the ratio of 2 is predicted for the biexcitons in a quantum-confined structure.[10,11]

Bacher *et al.* observed that the exciton lifetime was slightly shorter than the biexciton lifetime in single CdSe quantum dots, that is, $\tau_X/\tau_B \sim 1$.[12] According to their arguments, dielectric confinement in quantum dots enhances the Coulomb interaction among electrons and holes so that the biexciton state resembled the hydrogen molecule as a result of the spatial separation of the holes due to this enhanced Coulomb interaction. Thus, in a larger quantum dot, this molecular nature of the biexciton will be increased, which results in extending the biexciton lifetime. Although the actual diameter of CdSe/ZnSe quantum dots was estimated to be comparable to the exciton Bohr radius, the penetration of the exciton wave function into the barrier region effectively enlarges the dot size in the hard-wall potential approximation.[12] They concluded that the penetration of the exciton wave function and the disk shaped geometry of the quantum dot further reduced the ratio down to 1.

Taking $a_X \sim 10$ nm as the exciton Bohr radius in GaAs, the average diameter of our quantum dot sample is about five times larger than the exciton Bohr radius, that is, $d \sim 5a_X$. The effective diameter of our quantum dot in the hard-wall approximation will be larger than the actual diameter, thus the spatial separation of the holes in our quantum dot can be more pronounced compared with the case of Ref. 12. The estimated ratio of the lifetimes suggests that the biexciton state in our quantum dot sample should have more molecule-like characteristics than those of Bacher *et al.* due to the large quantum dot diameter.

The moleculelike nature of the biexciton allows us to take the effective molecule model by Citrin into consideration.[10] After Ref. 12, the biexciton wave function is given by the following expression in the limit of $\lambda \gg d \gg a_X$:

$$B_{2K} = \frac{1}{\sqrt{2}} \sum_k \{c_k X_{K+k} X_{K-k} + c_k^p X_{K+k}^p X_{K-k}^p\}. \tag{3}$$

The recombination probability of the biexciton is given by the next equation by taking into account the spin selection rule that prohibits the electron and hole with parallel spins from recombination,

$$\tau_B^{-1}(2K) = \sum_k |c_k|^2 \tau_X^{-1}(K-k). \tag{4}$$

The wave vector of the exciton left behind after the biexciton recombination is given by the recoil momentum of the emitted photon by the recombination. The exciton wave vector is larger than the inverse of the quantum dot diameter, *d*, due to the quantum confinement of excitons in the dot potential. On the other hand, the relative motion of the constituent excitons is typically bounded by the biexciton diameter, a_B. Therefore, the summation of c_k over *k* is scaled by a_B/d resulting in $\tau_X/\tau_B=|c_k|^2 \sim a_B^2/d^2$. The observed ratio of the lifetimes τ_X/τ_B can be consistently explained with the ratio $a_B/d<1$ because the exciton wave function may not penetrate much into the surrounding barrier material due to the deep confinement potential in our quantum dots sample. Santori *et al.* also estimated the ratio of the lifetimes with a relatively large InAs quantum dots where $d \sim 3a_X$; however, the ratio was estimated to be ~ 1.5.[9] This previously reported, relatively larger lifetime ratio can be explained by the weaker confinement of their quantum dot sample whose exciton resonance wavelength was close to the wetting layer level. The penetration of the wave functions into the barrier region was larger in these weak confinement quantum dots so that the ratio a_B/d can be larger than 1. The comparison of the quantum dot dimension and confinement energy shows that our estimated ratio of the biexciton lifetime to exciton lifetime is consistent with the previously reported values in the excitonic molecule model.

IV. CONCLUSIONS

We have measured the time dependence of the PL intensity of the exciton and biexciton from a single InAs/GaAs quantum dot. Rate equation analysis on the PL decays shows that the radiative lifetime of the biexciton is longer than that of the exciton. The rate equation analysis also explains the

fact that the PL intensity of the biexciton stronger than that of the exciton. These particular characteristics suggest that the biexciton has a moleculelike nature in the large quantum dots with deep confinement energy.

ACKNOWLEDGMENTS

The authors thank Hitoshi Yokota in the R and D Support Center, NEC Corporation, for his technical assistance.

*Electronic address: s-kouno@cq.jp.nec.com
†Present address: National Institute for Material Science, 1-1 Namiki, Tsukuba 305-0044, Japan.

[1] P. Michler, A. Imamoğlu, M. D. Mason, P. J. Carson, G. F. Strouse, and S. K. Buratto, Nature **406**, 968 (2000).
[2] C. Santori, M. Pelton, G. Solomon, Y. Dale, and Y. Yamamoto, Phys. Rev. Lett. **86**, 1502 (2001).
[3] D. Fattal, K. Inoue, J. Vuckovic, C. Santori, G. S. Solomon, and Y. Yamamoto, Phys. Rev. Lett. **92**, 037903 (2004).
[4] D. Fattal, E. Diamanti, K. Inoue, and Y. Yamamoto, Phys. Rev. Lett. **92**, 037904 (2004).
[5] S. A. Kaiser, T. Mensing, L. Worschech, F. Klopf, J. P. Reithmaier, and A. Forchel, Appl. Phys. Lett. **81**, 4898 (2002).
[6] K. Takemoto, Y. Sakuma, S. Hirose, T. Usuki, and N. Yokoyama, Jpn. J. Appl. Phys., Part 2 **43**, L349 (2004).
[7] K. Takemoto, Y. Sakuma, S. Hirose, T. Usuki, N. Yokoyama, T. Miyazawa, M. Takatsu, and Y. Arakawa, Jpn. J. Appl. Phys., Part 2 **43**, L993 (2004).
[8] T. Miyazawa, K. Takemoto, Y. Sakuma, S. Hirose, T. Usuki, N. Yokoyama, M. Takatsu, and Y. Arakawa, Jpn. J. Appl. Phys., Part 2 **44**, L620 (2005).
[9] C. Santori, G. S. Solomon, M. Pelton, and Y. Yamamoto, Phys. Rev. B **65**, 073310 (2002).
[10] D. S. Citrin, Phys. Rev. B **50**, 17655 (1994).
[11] T. Takagahara, Phys. Rev. B **39**, 10206 (1989).
[12] G. Bacher, R. Weigand, J. Seufert, V. D. Kulakovskii, N. A. Gippius, A. Forchel, K. Leonardi, and D. Hommel, Phys. Rev. Lett. **83**, 4417 (1999).
[13] L. Banyai, Y. Z. Hu, M. Lindberg, and S. W. Koch, Phys. Rev. B **38**, 8142 (1988).